CHANGES IN SUNSPOT AND FLOCCULAR SOURCES OF RADIO EMISSION PRECEDING AN IMPORTANCE 2N FLARE ON 23 AUGUST 1988

B. V. AGALAKOV, V. G. LEDENEV, B. I. LUBYSHEV, V. P. NEFEDYEV, S. A. YAZEV and G. N. ZUBKOVA
Institute of Solar-Terrestrial Physics, P.O. Box 4026, 664033 Irkutsk, Russia

A. KERDRAON
Observatoire de Paris, Section de Meudon, France

H. W. URBARZ†
Universität Tübingen, Astronomisches Institut, Aussenstelle Weissenau, 88214 Ravensburg/Rasthalde, Germany

(Received 23 May 1995; accepted 23 January 1997)

Abstract. Based on observations from the Siberian solar radio telescope, and invoking data from other observatories, we investigate preflare changes in the sunspot and floccular sources of radio emission and the development of an importance 2N flare in the chromosphere and corona in the active region on August 23, 1988.

It has been ascertained that preflare changes became observable six hours prior to the flare onset and manifested themselves in intense flux fluctuations above the sunspot and in an enhancement of the source emission flux above the flocculus.

It is shown that the flare onset is associated with a newly emerged magnetic flux in the form of a pore near the filament and with the appearance of radio sources above the filament. The flare was accompanied by type III radio bursts and a noise storm at meter wavelengths. Coronal mass ejection parameters are estimated from type III burst observations.

1. Introduction

Sources of the slowly varying component of solar microwave emission (S-component) and preflare variations in them have been and are among the most interesting objects of study. It is known (see, for example, Kundu, 1985; Gelfreikh, 1992) that S-component sources are rather complicated features consisting of several parts associated both with strong and compact sunspot magnetic fields and with extended and relatively weak magnetic fields of plages. Usually, separating sunspot and floccular sources and investigating them independently are difficult for several reasons. A most serious problem is the great brightness of the radio emission component associated with sunspots which plagues the investigation of less bright radio sources associated with flocculi, and the complexity of the spatial structure of the active region (AR).

In regard to the sunspot and flocculus components of radio emission during the development of the flare (radio burst), investigating them is difficult because the

† Deceased.

Solar Physics **173:** 305–318, 1997.

region generating the burst ‘screens’ to a significant extent (and often totally) the S-component sources in the AR. On the other hand, the S-component sources are a handicap to the study of the region generating bursts during the early stage of their development when the radio flux and brightness temperature of the burst generation region are significantly less than those of the S-component. Nevertheless, some progress has also been made in this area, with the advent of instruments affording high spatial resolution (Kundu, 1985).

In this paper, because of the extreme ‘simplicity’ of the NOAA 5115 active region spatial structure, we are able to carry out a separate study of radio sources associated with the sunspot and flocculus several hours prior to the onset and during the development of the flare on August 23, 1988. Furthermore, regions generating the burst did not coincide with regions of S-component sources, which enabled us to investigate their parameters during the stage of appearance and development of the burst. Based on sufficiently detailed chromospheric observational data available to us, we carried out a comparison of processes in the active region magnetosphere at levels where radio emission is generated, with processes occurring in the chromosphere.

2. Observations

This paper relies on observational data from the Siberian solar radio telescope (SSRT) operated by the Radioastrophysical Observatory of the Institute of Solar-Terrestrial Physics (Irkutsk), at 5.2 cm wavelength with angular resolutions ranging from 17$''$ in observations at local noon to 40$''$ at the beginning and end of the observations and, respectively, with time resolutions from 2.5 to 5 min; from the radio heliograph of the Meudon Observatory (Paris) at 164 MHz with an angular resolution of about 1 arc min; as well as from the spectrograph of the Astronomical Station at the University of Tübingen (Germany). The photospheric and chromospheric observations (at the center of the Hα line) were obtained at the Baikal Astrophysical Observatory of the Institute of Solar-Terrestrial Physics and at the Meudon Observatory.

2.1. Main peculiarities of the spatial structure of the S-component sources and of the region of generation of the burst

The burst and the importance 2N chromospheric flare under investigation (beginning 08:20 UT, maximum 08:48 UT) (*Solar-Geophysical Data*, 1989) occurred on August 23, 1988 in the AR NOAA 5115. An AR photoheliogram is presented in Figure 1(a). The AR NOAA 5115 showed an individual sunspot with the area of 140 $\times$ 10^{-6} hemisphere. The AR NOAA 5122 included a pore with an area of 21 $\times$ 10^{-6} hemisphere (*Solnechnye Dannye*, 1988). The flare had a typical two-ribbon structure (Figure 1(c), dotted contour). According to the duration of increasing brightness (from 30 to 50 min according to data from different observatories), it may be classified as a coronal flare (Slonim, 1973).

Figure 1(b) shows one-dimensional scan distributions of radio brightness for a time prior to the flare (first scan) and for the time of flare development (all subsequent scans). The radio brightness distribution before the flare shows two radio emission sources. Radio source A is identified with an individual sunspot AR NOAA 5115. Radio source B is identified with the brightest part of a diffuse extended flocculus, whose size at the time of the flare increased several times. Figure 1(c) (hatched region) shows the location of the flocculus maximum radio brightness.

The radio burst developed in a region without sunspots, between the sunspot and the flocculus, and had three regions of generation (in Figures 1(b) and 1(c), the are numbered 1, 2, and 3). One can see that the S-component source of the individual sunspot was quite well separated from regions of generation of the burst, which enabled us to analyze its behaviour at the time of flare development, and because the burst occurred at the end of the observation run at SSRT (it was preceded by observations during about six hours), long before the flare too.

Positions of brightness maxima of radio sources A and B were determined from one-dimensinal scans oriented at different angles. Simultaneous observations made with the south beam of SSRT, allowed us to determine the position of brightness maxima of the region of generation of the burst projected onto the AR chromosphere (shown by crosses in Figure 1(c)) with respect to the flare ribbons.

The objective of this paper is to examine the behaviour of the S-component sources prior to and during the flare, as well as the development of the radio burst in the lower and upper AR corona.

2.2. S-COMPONENT SOURCES PRIOR TO THE FLARE

Figure 2(a) shows a plot, illustrating a change in total radio flux (I) and circularly-polarized emission (V) of the S-component sources of the individual sunspot A (August 23). It is evident that during more than six hours before the flare the radio flux fluctuates dramatically and changes by about a factor of 3. The fluctuations in total radio flux were accompanied by almost synchronous oscillations of circularly polarized emission V. At instants of maximum flux values, the degree of polarization was about 30%. A decrease in radio flux was accompanied by an increase of the degree of polarization up to 40%.

Figure 2(b) gives a plot showing radio flux of this same source on the preceding day, August 22, when flares were missing from this AR. One can see that the flux remained almost unchanged during the observing run. On the strength of this, we believe that the fluctuations in radio flux of the sunspot source of radio emission (August 23) are a consequence of the processes occurring in the AR before the flare.

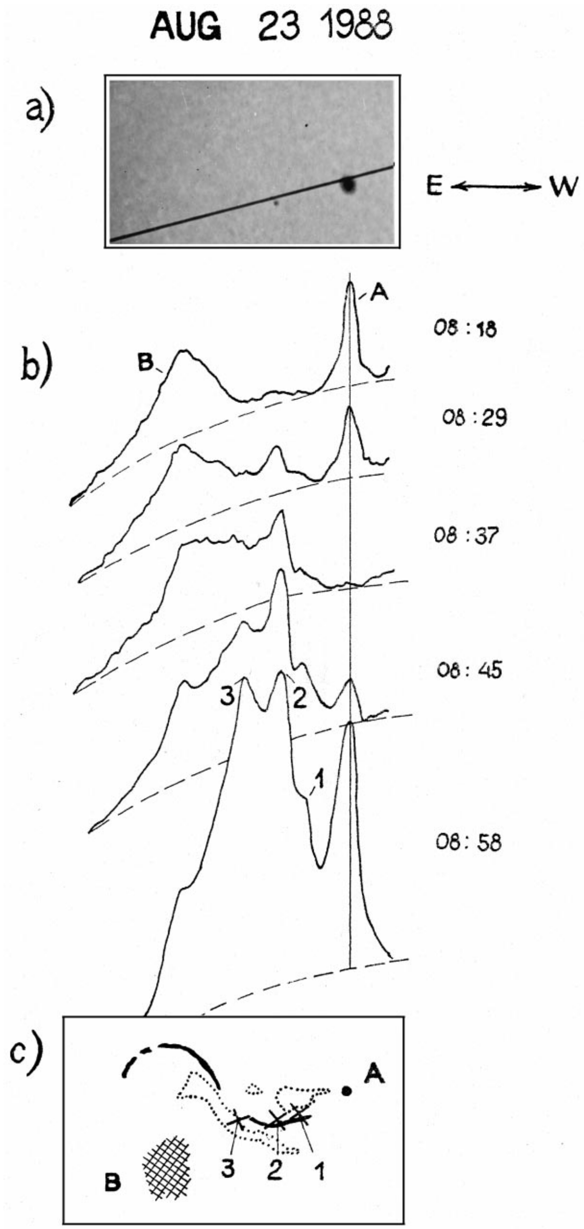

Figure 1. Chromospheric flare of importance 2N: (a) photospheric area at active regions 5115 and 5122; (b) series of radio brightness distribution scans at 5.2 cm wavelength: (A) radio source, associated with the sunspot of AR 5115; (B) associated with flocculus; 1, 2, 3 – burst radio sources; (c) a sketch of the chromosphere at a time close to maximum brightness of the chromospheric flare; heavy line – filament position; 1, 2, 3 – position of brightness centers of the burst-generating regions.

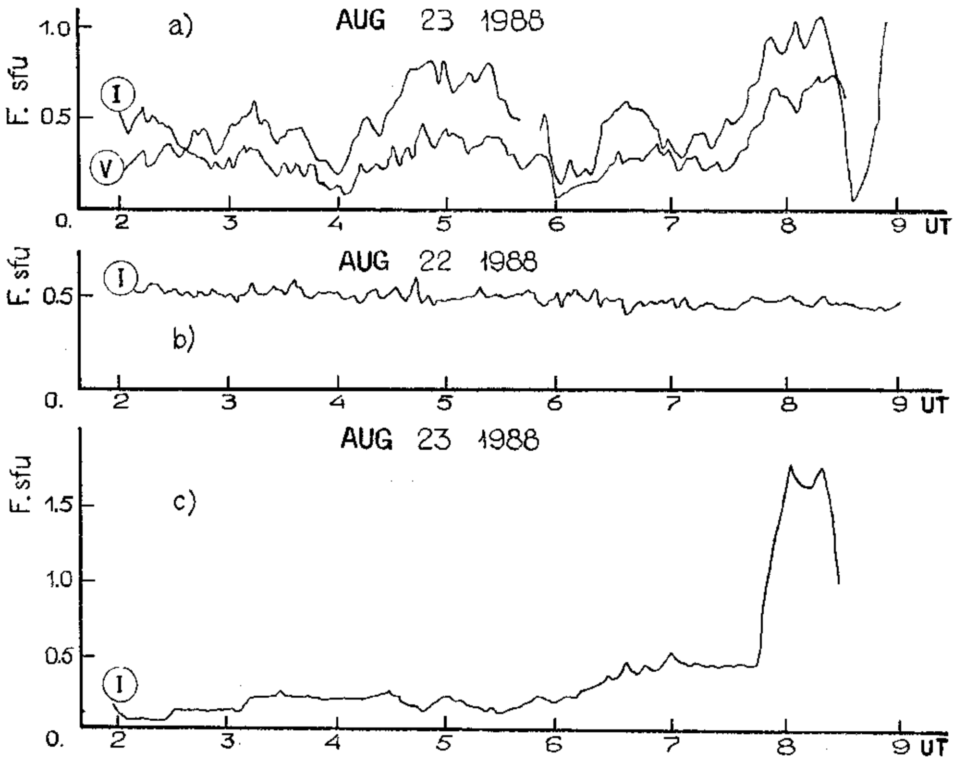

Figure 2. Changes in radio flux: (a) in total intensity (I) and circular polarization (V) of sunspot source A on 23 August, 1988; (b) in total intensity of sunspot source A on 22 August, 1988; (c) in floccular source B.

Brightness temperature at instants of maximum values of the radio flux on August 23 differed little from the brightness temperature of the source on August 22. What this means is that the radio flux fluctuations of the sunspot source (which we associate with the processes occurring prior to the flare) are a consequence of a decrease (rather than an increase) in brightness temperature because the changes in radio flux are unaccompanied by appreciable changes in the angular size of the radio source. This process begins to develop at least six hours before the flare onset.

A change in radio flux of the S-component located in the region of a diffuse flocculus (B) is shown in Figure 2(c). One can see that the radio flux from this source also varied during the observing interval at SSRT, but its changes were of a different character, namely insignificant fluctuations in radio flux before 05:30 UT, followed by an increase in radio flux. At the beginning of the observation, the radio emission region was about 50$''$ in size. Before the flare, it increased to 200$''$. The brightness temperature was rising and reached 70 000 deg by the flare onset.

2.3. S-COMPONENT SOURCES DURING THE DEVELOPMENT OF THE BURST. THE RADIO BURST DEVELOPMENT IN THE LOWER AND UPPER CORONA OF THE ACTIVE REGION

Figure 3 shows one-dimensional scans of the radio brightness distribution for the time of appearance and development of the generation of the burst. Designations for the S-component sources (A and B) and for regions of the generation of the burst (1, 2, 3) are the same as in Figure 1. One can see by their behaviour that the S-component sources A and B differ greatly. The radio source associated with the flocculus throughout the time interval during which it was quite well separated from the burst sources, remained almost unchanged. The same cannot be said of the sunspot source of radio emission. During the initial stage of development of burst-generating regions, it was decreasing, to disappear almost totally (08:37 UT) and appear again thereafter. The polarized emission source was changing in a similar manner.

The burst began to develop from compact source 2 (Figures 1 and 3) located near an individual pore (see Figure 1(a)). The pore appeared at least 2–3 hours before the flare onset. The source radio flux 2 during this evolutionary stage did not exceed 2 s.f.u. Its emission was markedly circularly polarized (30–40%). About 10 min later, two additional sources, 1 and 3, began to develop, and their emission was unpolarized.

Beginning at 07:30 UT, we have rather detailed chromospheric observations at the center of the Hα line taken at the Meudon Observatory. Fragments of these observations, shown in Figure 4, illustrate the development of a chromospheric flare and accompanying phenomena in the filament. The flare development was accompanied by the disappearance of the middle part of the filament and a bifurcation of its eastern (most distant from the sunspot) end, which was attended by the appearance of weak emission mottles in the chromosphere, resembling a ‘spray’.

A correlation made between chromospheric observations and observational data from SSRT lent support to our supposition of a relationship of brightness temperature fluctuations of the radio emission sunspot source with processes in the filament. The sunspot source brightness temperature was observed to decrease 10 –15 min after the middle part of the filament had disappeared. One of the most probable reasons for the decrease in brightness temperature of the sunspot source is the penetration of cold and dense filament material into the sunspot magnetic field, which led to shielding of the radio emission source. To the 10-min delay in the brightness temperature decrease of radio source A with the AR size of $\sim 10^5$ km there corresponds a velocity of ~ 100 km s^{-1}, equal in the order of magnitude to the sound velocity in the corona.

The evolving active process was accompanied by bursts in the meter wavelength range as recorded at the Radio Astronomical Station of the University of Tübingen (Germany). Two series of type IIIG and a continuum were observed. The first group of type IIIG bursts, observed in the interval 08:29:50–08:33:40 UT (see the

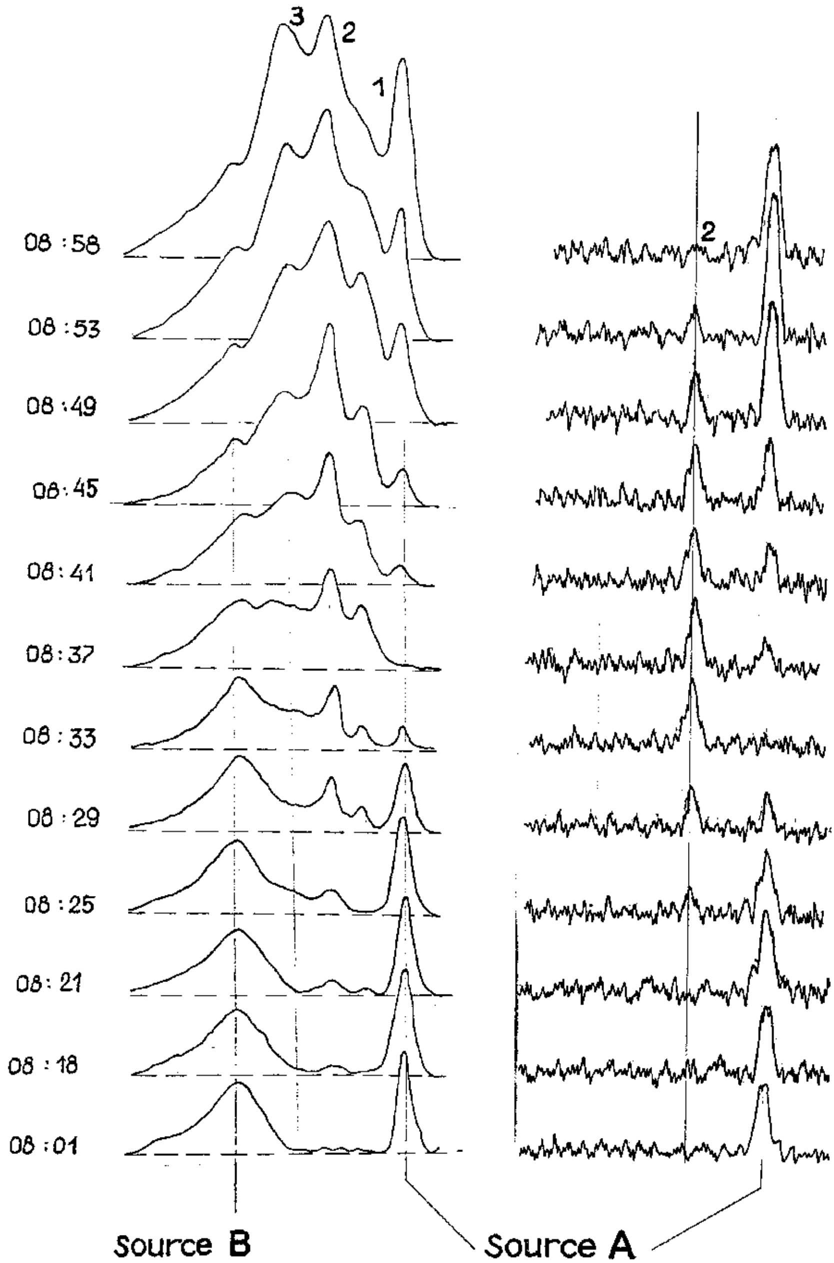

Figure 3. Series of scans of radio brightness distribution of total intensity (left scans) and circular polarization (right scans), showing changes of sunspot source A and burst radio sources (1, 2, 3) during the development of the chromospheric flare. The observing interval 08:18–08:41 UT includes the disappearance of the middle part of the filament and splitting of its eastern edge. The dashed lines indicate the quiet-Sun level.

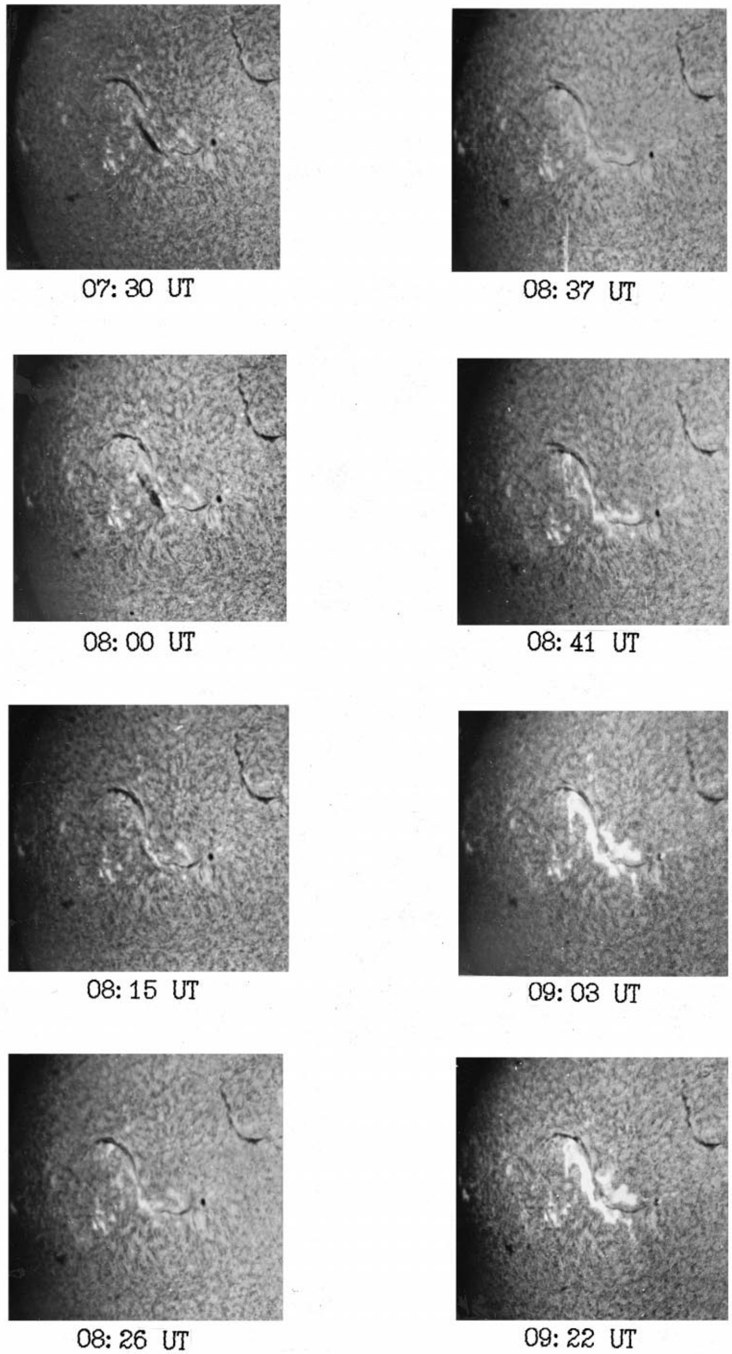

Figure 4. Change in the filament structure, and development of the chromospheric flare ribbons in the Hα line based on observations from the Meudon Observatory.

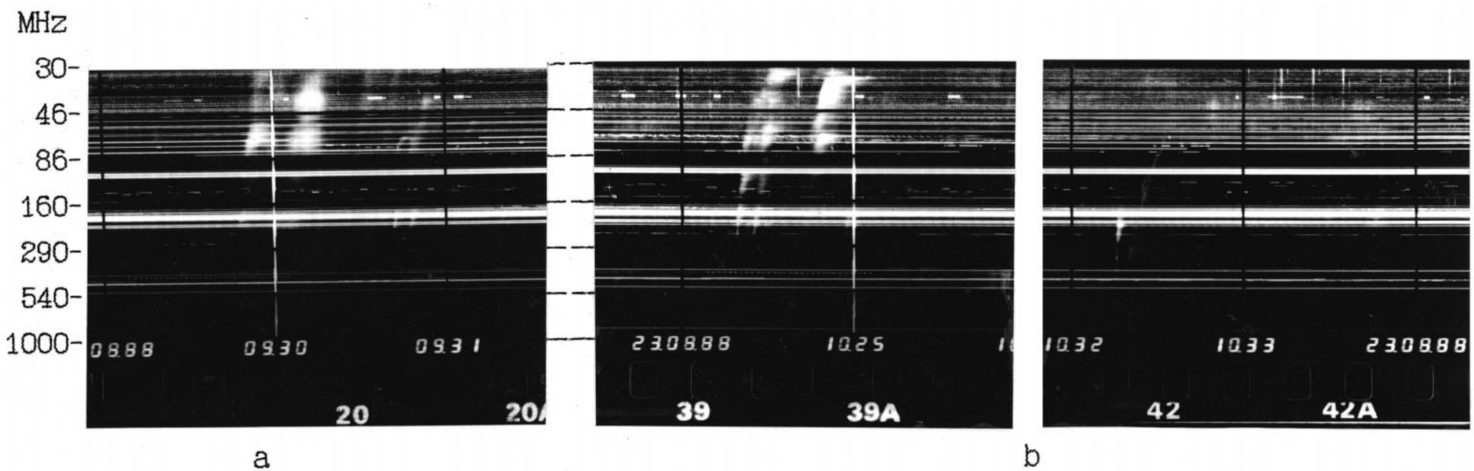

Figure 5. Spectrograms of type IIIG bursts: (a) first group; (b) second group. Time on the spectrograms: UT+1 hr. .

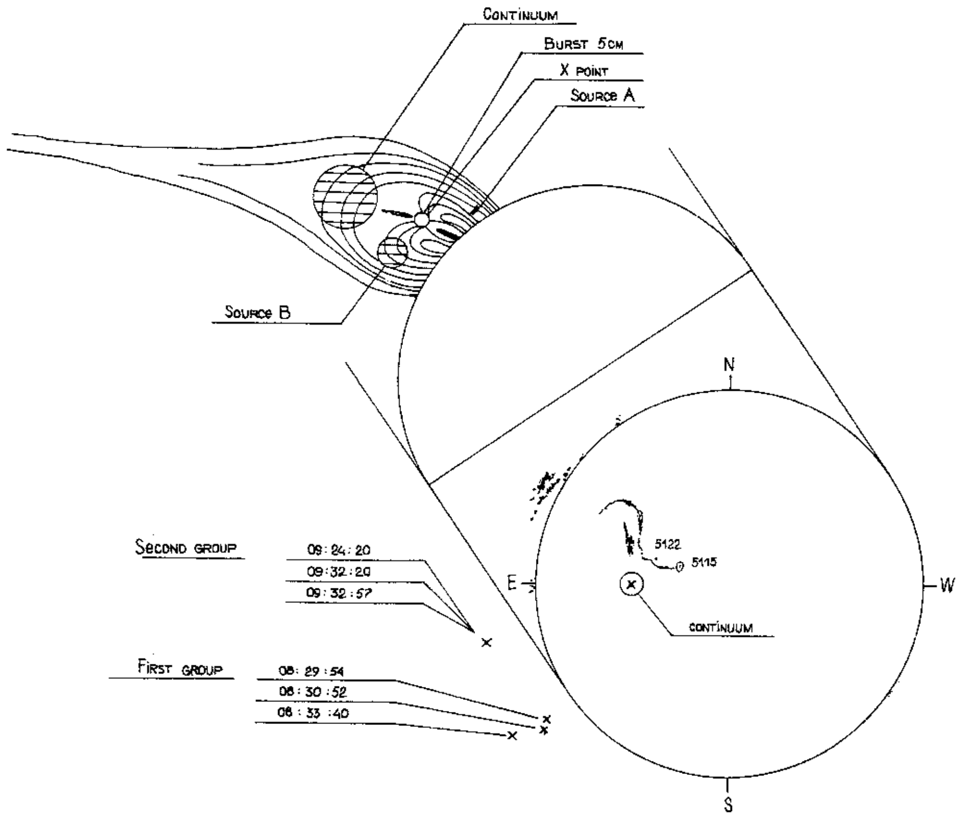

Figure 6. Magnetic field structure in active regions 5115 and 5122, and the position of the sources of microwave and meter emissions and the continuum in the tangent plane.

spectrogram in Figure 5), was time-coincident with the development of a compact burst generation region 2 located close by an individual pore. The other group of type IIIG bursts (beginning at 09:24:20) coincided with a recurring brightening of source 2. The beginning of the continuum emission, classified as type IIIN (08:40 UT), coincided with the beginning of development of burst generation region 3. The emission of this type reached a maximum at about 09:30 UT (almost simultaneously with the maximum of Hα emission and of radio flux at 5.2 cm) and lasted till 10:30–11:00 UT. The time of development of the type IIIN burst corresponds closely to that of the microwave burst. Thus, electrons that were responsible for the generation of groups of type IIIG bursts and the continuum originated from different generating regions.

Figure 6 shows the positions of regions generating type IIIG bursts and the continuum based on heliographic observations from the Meudon Observatory. The region generating the continuum is located much nearer to the region of Hα emission and centimeter emission, perhaps at the top of a closed AR magnetic field loop and, consequently, below the regions generating groups of type IIIG bursts (see Figure 5). The position of the regions generating type IIIG bursts of the first group shows distinctive dynamics. As time progresses, the generating region is moving away from the limb, unlike the regions generating type IIIG bursts of the second group, whose generating regions were virtually coincident.

That the region-generating type IIIG bursts of the first group is receding, bears witness to the fact that in the time between individual bursts the corona density in this region has increased substantially, i.e., a coronal mass ejection occurred. An upper bound to this ejection velocity can be inferred from the distance between the burst sources ($\sim$0.2 R) and from the difference of the observing times (about 3 min). Its value is about 800 km s^{-1}. This estimate agrees reasonably well with that obtained from SMM coronograph observations ($\sim$1000 km s^{-1}), according to which the coronal mass ejection was observed to occur above the limb during 08:53–10:36 UT (Burkepile and St. Cyr, 1993). Its maximum width was 125°. The ejection was shaped like a loop and was likely associated an expansion of the magnetic field loop structure. This is borne out by the presence of U-bursts, i.e., bursts that change, as time elapses, the sign of the frequency drift in groups of type III bursts (Figure 5). The ejection velocity is considerably higher than the sound velocity, hence it can be associated with a shock wave. Mass ejections into the corona are thought to be associated with type II and IV bursts. In the present case these two types of emission were not observed. Consequently, the ejection mass were not large, which agrees with the low intensity of the microwave burst.

Since the first group of type III bursts was observed before the coronal ejection appeared, this means that coronal material had begun to move as early as before the visible ejection arrived at the level of burst emission. This may be attributed to the fact that the coronal ejection boundary (the visible loop) corresponds to a contact discontinuity associated with the boundary of an expanding magnetic loop, and the migrating material ahead of it is a region behind the shock front associated with the expanding loop (Ledenev, 1980). The velocity of the shock front can be estimated on the assumption that the shock wave is generated at the flare onset time ($\sim$08:20 UT), and the first group of type III bursts was observed about 10 min later, at the distance of 0.5 R from the flare site in the tangent plane. Hence we get the shock velocity, $U_{sh} \geq 1200$ km s^{-1}.

Regions generating type IIIG bursts of the second group were observed at about the same distance from the disk center as was the last burst of the first group at 08:33:40 UT, but somewhat farther northward. Interestingly, the location of a subsequently observed weak type III burst (at about 09:23) was virtually coincident with that of a preceding group of bursts. That is to say that, by the time of the observation of the second group of type III bursts, the region at the level of emission of these bursts reached a stable state, such that energy release processes accompanied by type III bursts, cannot remove it from this state.

3. Discussion

According to the magnetogram presented in *Solar-Geophysical Data* (1988), radio sources identified with a sunspot and a flocculus, resided within opposite-polarity magnetic fields. The filament lay on the polarity inversion line of these magnetic fields. The magnetic field structure in the corona above the active region may schematically be represented (taking into account the ‘two-storey’ filament structure) as shown in Figure 6. The figure also marks the position of the radio sources discussed in this paper. The formation of a so-called X-point of the magnetic field is quite possible between the upper and lower parts of the filament.

Weak energy release processes occurring at the X-point introduce a change into the temperature regime in the upper part of the filament, which may be interpreted as the initial stage of its activation. It is known (Maksimov and Prokopiev, 1988; Schmieder, Fontenla, and Tandberg-Hanssen, 1991) that a change in the structure of the filament and the disappearance of its separate parts or of the entire filament was accompanied by drain of cold filament material along magnetic field lines downward. Part of the filament’s cold material enters the sunspot, giving rise to episodic decreases in its brightness temperature. It can be said that there is some periodicity in the decrease and recovery of the brightness temperature of the sunspot source with a period of 80–100 min. Oscillations with such a period are characteristic for line-of-sight velocities of prominences (filaments observed on the limb) (Bashkirtsev and Mashnich, 1991, 1993). This may be thought of as being indirect evidence that changes in brightness temperature are associated with filament activation processes. Such an interpretation is backed by the appearance in the chromosphere of point brightenings, having a ‘spray’ character, following the filament disappearance, which may be regarded as evidence for downward drain of material. The appearance of a similar emission like ‘spray’ following the filament disappearance was pointed out by Trifonov (1985).

About 2.5 hr before the flare, the energy release process develops a different character. This time is followed by an increase in temperature and size of the radio source in the floccular region (source B). About 40 min before the flare onset, the heating of the floccular source reaches a maximum. The energy release process associated with the heating process is taking place relatively far from the flocculus, above which lies the radio source. This follows from the fact that the flocculus remained unchanged during the flare.

The picture of flare development may be visualized as follows. Before an intense heating of the flocculus source (before 07:45 UT), the active region was in a metastable state. The flare onset is associated with emergence of new magnetic flux in the form of a pore near the filament. This field has a polarity opposite to that of the flocculus field, and its interaction with the flocculus field manifests itself as coronal heating above the flocculus and a filament destabilization. With the beginning of intense heating, which is evidenced by an increase in the size and brightness temperature of the flocculus radio source (source B), heat is being transferred along magnetic field lines to a region of the filament, predominantly to its upper part which is heated and becomes invisible as a consequence of a decrease in optical thickness. With filament heating, the system's equilibrium is upset, and the filament begins to expand, largely upward. Magnetic field lines that sustain the upper part of the filament begin to straighten themselves and shoot it upward. In this case, most of the prominence cold material is moving upward, which is confirmed by type III burst observations, and the other part of it travels along field lines to a region above the sunspot, thus leading to a decrease in the flux of the sunspot radio source and giving rise to emission in the chromosphere like a 'spray'. In the interface between the upper and lower parts of the filament (in the X-point region), a current sheet is formed, and the magnetic field reconnection process sets in, which is accompanied by still stronger heating and the appearance of burst generating regions at the place of the filament (sources 1, 2, and 3 in Figures 1 and 4). Thus, a key role in the flare development is played by the filament. It sustains the active region in a metastable state, thereby isolating opposite-polarity regions from each other, i.e., without permitting the magnetic field line reconnection process to evolve. But as soon as the filament is removed from the equilibrium state, it stops performing a protective function, and a flare sets in.

An intense reconnection process and a heating of the region above the filament continued till 09:24 UT; following an abrupt energy release process, accompanied by a group of typ III bursts, the process began to decay. Energy release continued also during the decay phase, as witnessed by the long persistence of the noise storm source in the meter wavelength range.

4. Conclusions

It follows from the foregoing discussion that: (1) In the flare observed, the preflare energy release process begins at least six hours before the flare onset. (2) This process begins to proceed most intensely 2.5 hr before the flare. (3) The flare is initiated by emergence of a new magnetic field which removes the filament from the equilibrium state. Changes taking place in the filament play a key role in the flare development. (4) High-spatial-resolution observations at meter wavelengths make it possible to gauge, from the displacement of the type III emission source at fixed frequency, the presence of a mass ejection from the flaring region and deduce its velocity.

Acknowledgements

This work has been done under financial support from the Russian Foundation for Fundamental Research (project code 93–03–3106) and the 'Astronomy' Foundation (project code 8–276).

We are grateful to Mr V. G. Mikhalkovsky for his assistance in preparing the English version of the manuscript.

References

Bashkirtsev, V. S. and Mashnich, G. P.: 1991, *Astron. Astrophys.* **91**, 93.

Bashkirtsev, V. S. and Mashnich, G. P.: 1993, *Astron. Astrophys.* **279**, 610.

Burkepile, J. T. and St. Cyr, O. C.: 1993, *Catalogue of Mass Ejections Observed by the SMM Coronograph*, Boulder, Colorado.

Gelfreikh, G. B.: 1992, in R. F. Domly (ed.), *Solar Radio Emission at Centimeter Wavelengths*, Proceedings of the Workshop on the Solar Electromagnetic Radiation Study for Solar Cycle 22, p. 196.

Kundu, M. R.: 1985, *Solar Phys.* **100**, 491.

Ledenev, V. G.: 1980, *Astron. Zh.* **57**, 113.

Maksimov, V. P. and Prokopiev, A. A.: 1988, 'Some Processes at the Filament Branch Point', *Issledovaniya po geomagnetizmu, aeronomii i fizike Solntsa*, Nauka, Moscow, Vol. 79, p. 90.

Schmieder, B., Fontenla, J., and Tandberg-Hanssen, E.: 1991, *Astron. Astrophys.* **252**, 343.

Slonim, Yu. M.: 1973, in Yu. M. Slonim (ed.), 'Solar Flares and Processes in Active Region', *Solar Processes and Their Observation*, FAN, Tashkent, p. 3.

Solar-Geophysical Data: 1988, No. 530, Part I, Boulder, Colorado.

Solar-Geophysical Data: 1989, No. 534, Part II, Boulder, Colorado.

Solnechnye Dannye: 1988, No. 8.

Trifonov, V. D.: 1985, 'Structural Features of a Large Prominence-Filament in June–July of 1982', *Issledovaniya po geomagnetizmu, aeronomii i fizike Solntsa*, Nauka, Moscow, Vol. 72, p. 172.

Yazev, S. A., Zubkova, G. N., Nefedyev, V. P., and Lubyshev, B. I.: 1990, *Solnechnye Dannye* No. 6, 76.